Univerza
v Ljubljani
Fakulteta
za gradbeništvo
in geodezijo

Jamova cesta 2
1000 Ljubljana, Slovenija
http://www3.fgg.uni-lj.si/

University
of Ljubljana
Faculty of
Civil and Geodetic
Engineering

Jamova cesta 2
SI – 1000 Ljubljana, Slovenia
http://www3.fgg.uni-lj.si/en/

Žnidarič, A., Turk, G., Zupan, E. 2015. Determination of strain correction factors for bridge weigh-in-motion systems. *Engineering Structures* 102 (2015) 387-394. DOI: 10.1016/j.engstruct.2015.08.026.

Determination of strain correction factors for bridge weigh-in-motion systems

A. Žnidarič[a], G. Turk[b], E. Zupan[a*]

[a] Slovenian National Building and Civil Engineering Institute, Dimičeva 12, SI-1000 Ljubljana, Slovenia

[b] University of Ljubljana, Faculty of Civil and Geodetic Engineering, Jamova 2, SI-1115 Ljubljana, Slovenia

Abstract

The paper presents an automatic procedure for the correction of bridge weigh–in-motion (B-WIM) measurements, which are used to determine the axle loads of heavy vehicles using instrumented bridges. According to the European Specifications for Weigh-in-Motion criteria, using this procedure the weighing results could be improved by up to one accuracy class. Whereas measurements performed on steel structures provide reliable information about the global behaviour of individual bridges, which is accounted for in the B-WIM algorithms, cracks that are present in concrete structures can, depending on their locations with respect to installed strain transducers, amplify or reduce the response. In the present work special care was taken to detect and calibrate any strain transducer which showed a disproportional response. The accuracy of the method was investigated numerically in relation to the extensive data which were available in the case of a

* Corresponding author. *Email address:* eva.zupan.lj@gmail.com

reinforced concrete bridge (motorway underpass), located near Ljubljana, Slovenia, and then validated by a one-to-one comparison of the B-WIM weighing results and the statically weighed test vehicles.

Keywords:

WIM – weigh-in-motion, bridge response, strain gauges, nonlinear regression, correction of measurements

---

1 Introduction

Weighing of vehicles in motion is an important source of reliable traffic loading information, which can be used to support infrastructure management ([1], [2], [3]), traffic policing, and vehicle weight enforcement [4]. For this purpose, some countries use static weigh stations. However, such solutions are space demanding, interrupt the flow of traffic, introduce delays into the transportation network, and are expensive to operate. If vehicle weight enforcement is the primary reason for static weighing, which is common in many countries around the world, then it is likely that the resulting data will not provide useful insight into the traffic loading on specific road sections.

The most common and effective alternative to static weighing consists of weigh-in-motion (WIM) systems. Since they weigh vehicles at highway speed they are less accurate than their static alternative, but they have the advantage of being able to capture the entire traffic flow on a road section. Two main families of WIM systems exist [5]: pavement WIM systems, and bridge (B-WIM) systems. Since early days, pavement systems have been the dominant group of devices on the market. They measure wheel loads by means of weighing detectors of different technologies that are embedded into the smooth road surface. In most cases the width of the sensors is less than the footprint of a tyre. For this reason accurate velocity measurements are needed in order to integrate the sensor responses into the axle loads [5]. Being under the direct pressure of tyres, pavement WIM

systems can deteriorate relatively quickly, as does the pavement. This changes its smoothness and directly affects the accuracy of the results obtained. On the other hand, the main idea of B-WIM systems is to put most of the measurement devices under the bridge [6], [7]. In early years axle detectors were needed on the road surface to capture information about vehicle velocity and axle configurations [8], but over the last decade these have been almost completely replaced by sensors that are placed under the bridge. Although such a *Free-of-Axle Detector* (FAD) set-up provides less precise information about the axles of vehicles, having all the sensors removed from the road surface greatly improves the durability of installation, and reduces traffic delays during installation and maintenance.

Bridge WIM (B-WIM) systems use instrumented bridges to weigh vehicles at highway speeds. The basic principle has not changed for over 30 years [9]. A bridge is instrumented with strain transducers and in some cases other additional sensors which measure the bridge response caused by heavy vehicles driving over it. During the first 20 years of their existence, and with the exception of a simpler version which was widely used in Australia [10], B-WIM systems were not important players on the market. However, in more recent years considerable progress has been made. Since the first attempts by Moses [9], some intensive research has been performed over the last two decades, see [3], [5], [11], [12], [13], [14], [15], [16] and [17]. As a result B-WIM systems have been improved up to the point where they can compete successfully with pavement systems. Today B-WIM systems can be applied to most types of bridges (beam and slab, or slab only, integral or simply supported, culverts to long span bridges, etc.) as long as the effective influence lines used for weighing are shorter than about 40 m [18]. A number of different algorithms have also been developed (using full dynamic bridge-vehicle interaction [19], MFI – Moving Force Identification [20], wavelets [21], and multiple-sensors, etc.), but they have not yet been implemented in any commercially available B-WIM system.

The algorithms for post-processing the measured response of WIM systems are based on

the classical theory of elasticity. The axle loads are sought by minimising the difference between the calculated bridge response, obtained by superimposing the influence lines multiplied by the unknown axle loads, and the measured strain response. This proved to be an efficient procedure for most structures that were analysed. These algorithms have been well optimised, and further improvement of the accuracy of weighing results can only be sought for in the development of advanced procedures for processing the recorded data, and in better calibration of the structural parameters such as the influence lines.

After the raw signal has been smoothed and filtered by standard mathematical tools, the recorded responses of the sensors, which are placed in line orthogonally to the driving direction (Figure 1, right), should capture the distribution of strains across the bridge. This is not always true as the gauge factors may vary from one sensor to another. This can be mostly attributed to differences in the quality of sensor production and the precision of their installation, particularly the exact orientation of the gauges. Certain corrections of gauge factors can compensate for such irregularities, and reduce the errors in weighing results. Such corrections were initially performedin a heuristic trial-and-error method. Although the results were, in most cases, satisfactory, there is a clear demand for the automated calculation of sensor correction factors.

By means of the proposed procedure sensors with disproportional responses, which are caused by different sources of imperfections, can be detected and calibrated in order to achieve higher quality input for the B-WIM measurements and it should be possible for it to be applicable to various arrangements of sensors on slab bridges. Its effectiveness is demonstrated by the example of a reinforced concrete slab bridge (forming a motorway underpass). Static weighing results were used to validate the method, which is, however, limited to transversely symmetrical bridges with more than one driving lane.

2 Definition of the problem

Regardless of the algorithm used, today most B-WIM systems process the results of strain measurements recorded at times of vehicle crossings, and convert this information into axle loads. In the case of steel girders, and sometimes also in the case of steel reinforcement, strains can be measured by means of strain gauges, but in most cases detachable strain transducers have to be mounted onto the soffit of the bridge superstructure. An example of two different types of installation is shown in Figure 1.

Figure 1: Strain gauges installed on a steel orthotropic-deck bridge (left), and a typical strain transducer set-up on a reinforced concrete bridge (right).

A properly set-up and calibrated B-WIM system should be able to measure the realistic response of bridges under vehicle loadings, and thus yield axle loads that are within a few percent of their statically weighed values [22]. Yet, experience has show that, particularly in the case of reinforced concrete bridges, the achieved accuracy is frequently unsatisfactory. One of the main reasons for this is that the strain sensors do not necessarily provide the information which is expected (i.e. the global bridge response/strains under vehicle loadings). Whereas strain gauges installed by experienced technicians can, in most cases, measure strains that comply with the assumptions of the B-WIM algorithm, the quality of the output from strain transducers is less consistent since it depends on two important factors:

i) The transducers are fixed to the bridge either by means of 2.5 cm long steel anchors which are drilled into the concrete, or else to mounting plates that are glued onto the

concrete or steel surface. The sensors are then secured by bolts with washers, which, depending on the skill and consistency of the technician, can significantly affect the measured signals.

ii) Reinforced concrete structures are frequently not completely intact, and usually exhibit a considerable number of cracks. Most of them are very thin, and are difficult to detect and avoid during the installation process. Thus, instead of measuring the global strains of the structure as expected by the B-WIM algorithm, a strain transducer may record a local strain response. Based on the authors' experience, and the results of performed measurements, such a response can, in the case of reinforced concrete structures, be up to 4 times greater if the sensor is installed across a crack, or equal to only about one quarter of the expected value if there is a crack just outside the sensor.

Finally, the locations of the sensors, as well as the quality of their production and to some extent their malfunctioning (calibration which fades over time), can have similar negative effects that have to be accounted for.

A typical response that was recorded by means of the B-WIM system which is installed on a reinforced concrete integral slab bridge (an underpass) with a 6.0 m span that is located on the A2 motorway near Ljubljana, Slovenia, is presented in Figure 2. Twelve equally spaced strain transducers were located under the bridge in order to measure its response beneath the two driving lanes and the hard shoulder (Figure 1, right). The average maximum amplitudes of the individual strain transducer responses, calculated from over 4 months of traffic (approximately 150 thousand heavy vehicles), are shown beneath the slab in Figure 2. To obtain this diagram, the raw responses due to the vehicles in one lane only (without multiple-presence events) were first processed by standard mathematical procedures in order to remove the high frequency noise. Then, before averaging, the response of each individual event (the driving of a single heavy vehicle over the bridge) was normalized so that the sum of the responses of all twelve sensors was equal to one.

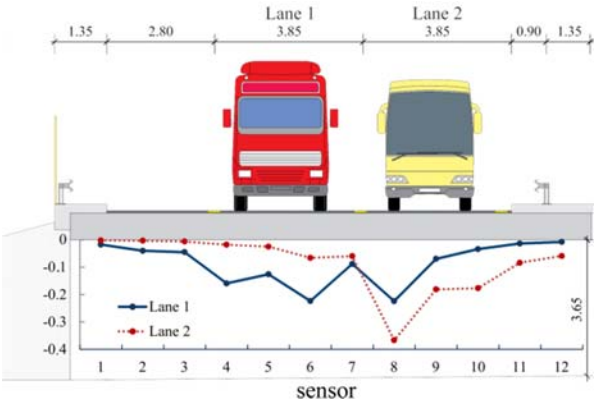

Figure 2: Cross section of one half of the investigated motorway slab bridge, showing the average responses of all twelve strain transducers.

Clearly, the measured response in Figure 2 does not match the anticipated transverse distribution of strains in a slab [23], from which the average lateral positions of the vehicles should be evident. In this case the maximum response was detected by sensor number 8 regardless of whether vehicles were driving in the main lane or in the overtaking lane. A subsequent check revealed that this transducer had been positioned over a 0.2 mm wide crack. It will be shown later that the overlooking of such damage can have a significant effect on the accuracy of the B-WIM measurement results, particularly if multiple-presence events, with vehicles in more than one lane at the same time, need to be successfully accounted for [24].

The development of an algorithm for the automatic detection of correction factors is based on the assumption that the response of the structure is similar for all types of conventional heavy traffic, i.e. that the response of the transducers depends linearly on the total weight of a vehicle on the bridge. The validity of this assumption can be statistically confirmed. The complete set of collected normalized data (382 823 trucks on the 1st lane and 23 478 trucks on the 2nd lane) was divided into five classes, separately for each lane, depending on the level of maximum measured strain. The averaged responses were evaluated for each class separately. Boundaries between individual classes were selected at every 20th percentile of the maximum strains, which means that each curve represents the average values of 76 564 vehicles in lane 1 and 4 696 vehicles in lane 2

(Figure 3). The curves are almost identical, which confirms the validity of the assumption that the observed anomaly does not depend on the level of loading. The differences are slightly greater in lane 2, which can be explained by the considerably smaller size of the sample.

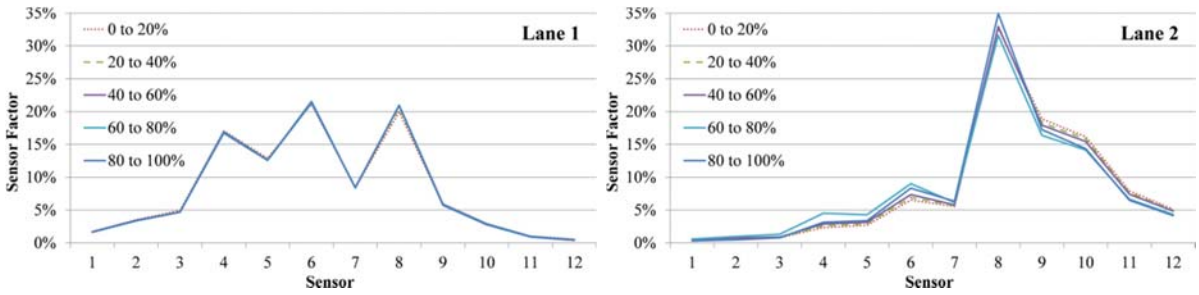

Figure 3: The five classes of maximum measured strain for each lane: the average response of the normalized measurements.

3 Procedure for the determination of optimal correction factors

In this chapter the theoretical background of the method is presented and illustrated by means of an example.

3.1 Primary definitions and assumptions

Let $S_1, S_2, \ldots, S_N$ denote the responses of N collinear strain sensors positioned at distances $x_1, x_2, \ldots, x_N$ from the edge of the bridge. We need to determine coefficients $k_1, k_2, \ldots, k_N \geq 0$ in such a manner that the corrected strain response

$$\tilde{S}_1 = k_1 \cdot S_1, \tilde{S}_2 = k_2 \cdot S_2, \ldots, \tilde{S}_N = k_N \cdot S_N \quad (1)$$

leads to accurate values of the vehicle/axle weights.

The solution of the task should be based on earlier experience as well as on the properties of the bridge. For this reason a short monolithic slab bridge was investigated, so that it can be assumed that, due to the constant cross section and boundary conditions, the average of the corrected responses for the driving and overtaking lanes should be similar. An even more important assumption is concerned with the expected response of the structure: the

largest response of the structure should be recorded under the vehicle, i.e. under its wheels, and should decrease as the distance from the wheel increases. The model describing the relationship between the lateral coordinate of the sensor and the response is clearly nonlinear. In order for a model to be applicable to day-to-day B-WIM measurements, it is of the greatest importance that it should be, on the one hand, sufficiently simple, while simultaneously fitting both the empirical and theoretical results well. Although the dynamic response is measured, by means of numerical studies it has been observed that a quadratic or even higher-degree polynomial is not the most appropriate. Thus, the proposed model is based on a linear combination of a Gaussian function, a constant, and a linear term. Formally, the model is defined in two manners; (i) for the generalized response of a bridge under a vehicle it is assumed that

$$f(x;\beta_1,\beta_2,\beta_3,\beta_4) = \beta_1 + \beta_2 x + \frac{1}{\beta_4\sqrt{2\pi}}\exp\left(-\frac{1}{2}\left(\frac{x-\beta_3}{\beta_4}\right)^2\right), \tag{2}$$

and (ii) in the case of a more detailed consideration of two wheels acting at the same lateral position that

$$g(x;\beta_1,\beta_2,\beta_3,\beta_4) = \beta_1 + \beta_2 x + \frac{1}{2\beta_4\sqrt{2\pi}}\left(\exp\left(-\frac{1}{2}\left(\frac{x-\beta_3-1.05}{\beta_4}\right)^2\right) + \exp\left(-\frac{1}{2}\left(\frac{x-\beta_3+1.05}{\beta_4}\right)^2\right)\right), \tag{3}$$

where $x \in [x_1, x_N]$, and β_1 - β_4 have to be estimated from the sample. Without the first two terms, β_3 and β_4 would describe the mean and the standard deviation of the sample. However, such a model would be restricted to the unit L_2 norm. To overcome this constraint the terms with β_1 and β_2 are added, which permit non-unity and linear dependency to be incorporated into the model. Note that the measured data have already been subjected to a normalization procedure during the pre-processing of the signal. A small but important contribution of the first two terms can therefore be expected from (2), whereas the Gaussian part of (2) - the density function of the normal distribution - makes a major contribution to the shape of the response curve. The parameter β_4 also

serves for the calibration of the generalized response function f. The coefficients $\beta_1 - \beta_4$ in Equation (3) have a similar role as in Equation (2). In the case of the more detailed response (3), the expected shape due to point loads at the positions of the wheels is taken into account, allowing the function g to have two separate peaks. The value 1.05 represents one half of the distance (in meters) between the centres of tyres on an average axle of a heavy commercial vehicle. This enforces the occurrence of peaks at a distance corresponding to the truck width. Due to normalization of the measured response, the L_2 norm of g should still have a value close to unity. This is why the third term in (3) represents the average value of the two Gaussian functions.

Note that the more detailed shape function should provide better results, but only if the sensors are placed closely enough together with respect to the truck width, which for practical reasons (the limited number of available measurement channels) is not always feasible. Sparser placement of sensors also means that any malfunctioning of the sensors will be more difficult to compensate for.

3.2 Correction factors of the measured response: the basic procedure

All the numerical investigations were performed on data that were recorded by the B-WIM system installed on the bridge VA0028 [17]. The system consists of twelve sensors at centre-to-centre distances of 1.05 m. In order to provide an input for the proposed correction, the load distribution factors were computed for data recorded in August 2013, when the system captured 29 788 events with vehicles having a gross weight of more than 3.5 tons (trucks) in the driving lane (Lane 1), and 779 in the overtaking lane (Lane 2). Validation of the coefficients was performed on the 62 vehicles that were weighed statically during the period between September 2013 and June 2014.

The numerical analyses presented here were performed in a Matlab computing environment [25]. Non-linear regression [26] was first run for each event, which can generally be described as a procedure where in the case of each event t_i ($i = 1, 2, \ldots, M_1 + M_2$, and M_1, M_2 are the numbers of events in the driving and overtaking lanes,

respectively) we seek for such parameters $\beta_1(t_i), \beta_2(t_i), \beta_3(t_i)$, $\beta_4(t_i)$ which would result in the best fit between the responses $S_1(t_i), S_2(t_i), \ldots, S_N(t_i)$ and the regression function (2) is based on the least square method. Note that the detailed shape function (3) could also have been applied, but it was found to be unsuitable for the available data due to the disproportional measurements provided by one sensor, which will be further discussed in the following section. As the problem is nonlinear an iterative procedure is needed. At each t_i the quotients:

$$k_j(t_i) = \frac{\tilde{S}_j(t_i)}{S_j(t_i)}, \text{ for } \tilde{S}_j(t_i) = f(x_j; \beta_1(t_i), \beta_2(t_i), \beta_3(t_i), \beta_4(t_i)) \quad (4)$$

which serve for the calibration are evaluated. The data were assembled and the results were computed separately for each lane. The average values of $k_j(t_i)$ for all events t_i were then evaluated for each lane in order to obtain the coefficients $\overline{k}_j^1$ and $\overline{k}_j^2$ for each strain sensor. They are presented, for the given example of bridge VA0028, in Table 1.

Table 1: Average scaling coefficients k_j for both lanes obtained by nonlinear regression applying Equation (2).

Sensor j	1	2	3	4	5	6	7	8	9	10	11	12
$\overline{k}_j^1$	1.31	1.07	1.51	0.70	1.257	0.81	1.94	0.60	1.47	1.30	1.50	0.86
$\overline{k}_j^2$	0.64	0.12	0.42	0.27	0.68	0.89	2.66	0.71	1.50	0.98	0.88	0.44

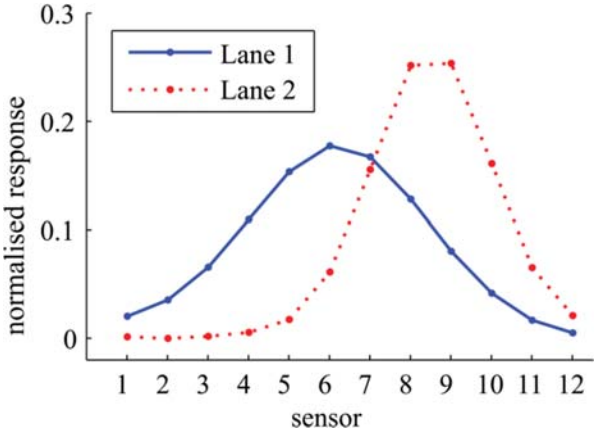

Figure 4: Corrected response for the two lanes.

In the following, the upper indices 1 and 2 denote the two driving lanes of the bridge.

Finally, the similarity of the two curves is checked. Figure 4 presents the average corrected responses $\overline{\tilde{S}}_j^1$ and $\overline{\tilde{S}}_j^2$ of each lane, separately, after the correction factors $\overline{k}_j^1$ and $\overline{k}_j^2$ have been applied:

$$\overline{\tilde{S}}_j^1 = \frac{\sum_{i=1}^{M_1} \overline{k}_j^1 \cdot s_j^1(t_i)}{M_1}, \quad \overline{\tilde{S}}_j^2 = \frac{\sum_{i=1}^{M_2} \overline{k}_j^2 \cdot s_j^2(t_i)}{M_2}. \tag{5}$$

It is clear that the obtained curves, while being much smoother than the originals, are still less similar than expected. On a bridge with a constant cross-section across its whole width, as in this example, it could be expected that the response in the two lanes would be similar with respect to height and width, and that the strains would be dispersed transversely in similar ways. Naturally, differences cannot be avoided towards the two free edges of the slab, but these sensors are less important for weighing, and contribute considerably less to the accuracy of the results.

In order to be able to assess the similarity of the two curves a numerical algorithm is needed. The difference between the average fitted responses for each lane was determined by comparing the parameters corresponding to the approximation of the response curves shown in Figure 4.

Table 2: Comparison of the corrected responses between the two lanes.

$\tilde{\beta}_4^1$	$\tilde{\beta}_4^2$	$\lvert\tilde{\beta}_4^1 - \tilde{\beta}_4^2\rvert/\tilde{\beta}_4^1$
0.30870	1.51780	0.34258

Note that the individual $\overline{k}_j^{\alpha} \cdot S_j(t_i^{\alpha}), j = 1, .., N$, at fixed events t_i^{α}, for $\alpha = 1, 2$ corresponding to both lanes are exactly the function values f at x_j for parameters $\beta_1(t_i^{\alpha}), \beta_2(t_i^{\alpha}), \beta_3(t_i^{\alpha}), \beta_4(t_i^{\alpha})$ in accordance with our model (2). This stems directly from Equation (4). After averaging, the mean values $\overline{\tilde{S}}_j^1$ and $\overline{\tilde{S}}_j^2$ cannot be obtained directly from Equation (2), but they are very close to the values of our model at each node x_j for some parameters $\tilde{\beta}_1^1 - \tilde{\beta}_4^1$ and $\tilde{\beta}_1^2 - \tilde{\beta}_4^2$, respectively. This is due to the small variation of the coefficients $\overline{k}_j^1$ and $\overline{k}_j^2$. Consequently, the same shape function will be used to approximate the average curves in Figure 4. The nonlinear regression-based fitted parameters from model (2) will be denoted by $\tilde{\beta}_{\mathrm{i}}^1$ and $\tilde{\beta}_{\mathrm{i}}^2, \mathrm{i} = 1, \ldots, 4$. The parameters $\tilde{\beta}_4^{\alpha}$ determine the 'width of the bell' of the model based on the probability density function of normal distribution. From Table 2 only a low degree of similarity can be observed between the two curves since the relative difference between the two parameters (34%) is relatively large.

3.3 Detection and calibration of a sensor with a disproportional response

The reason for the low degree of similarity between the results for the two lanes is that any sensor can provide values that are far from the expected ones. This could be due to a faulty sensor or, as in the present example, a crack in the concrete located between the anchors of the sensor. In order to identify a sensor providing disproportional signals it is necessary to repeat the basic procedure from Section 3.2 N times, and for each repetition to leave out the measurements of one sensor. For example, in the l^{th} calculation the measurements $S_1, \ldots, S_{l-1}, S_{l+1}, \ldots, S_N$ are accounted for by the calculation of $N - 1$ coefficients $k_{j,j\neq l}$ of the strain sensors positioned at lateral positions

$x_1, \ldots x_{l-1}, x_{l+1}, \ldots, x_N$. The results of the standard deviations $\tilde{\beta}_4$ for each lane and the relative absolute differences between the lanes for these *N* calculations are assembled in Table 3.

Table 3: Comparison of the driving and the overtaking lanes; the correction coefficients and responses were computed without considering the data of one sensor.

excluded sensor	$\left\|\tilde{\beta}_4^1 - \tilde{\beta}_4^2\right\| / \tilde{\beta}_4^1$
1	0.34533
2	0.34470
3	0.35829
4	0.33072
5	0.31183
6	0.41785
7	0.27471
8	**0.04975**
9	0.69248
10	0.35371
11	0.35913
12	0.36244

Figure 5 presents a few corrected responses that fit the model, but they were computed without considering the data recorded by the second, fifth, eighth, and eleventh sensor, respectively. From Table 3 and Figure 5 it can be seen that the resemblance between the curves increases dramatically if the data recorded by the malfunctioning 8th sensor are eliminated. The calculation excluding the 8th sensor gives eleven values $k_{j,j\neq 8}$ for each of the two lanes, see Table 4. They serve as the most appropriate basis for the determination of the final correction factors.

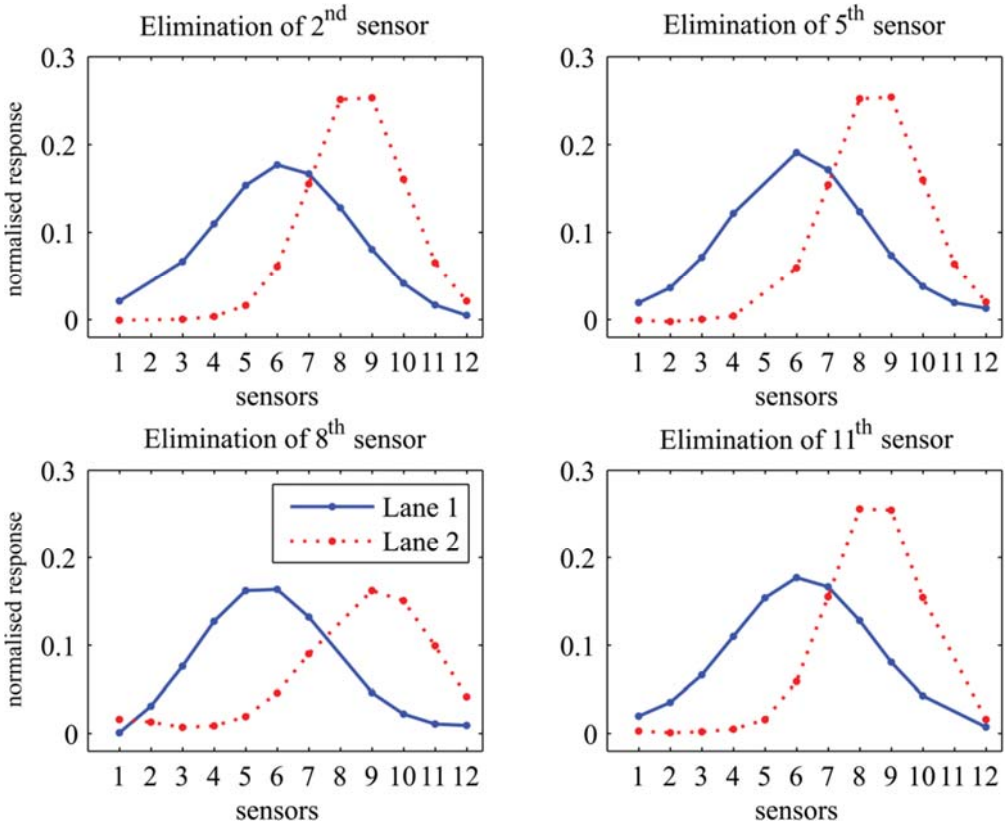

Figure 5: Average corrected responses; the correction factors are computed from the original data without considering one sensor.

Now the individual coefficients for the eleven sensors have to be evaluated, independently of the driving lane. They are obtained by averaging the coefficients $k_{j,j\neq 8}$ for the two lanes. The exceptions to this rule are sensors 1 and 2, where the coefficients derived from lane 1 were assumed. From Table 4 a higher discrepancy can be observed between the two coefficients, and from the graph entitled 'Elimination of 8th sensor' in Figure 5 it is clear that the corrected response of the first two sensors in lane 2 (shown by a dotted line) is higher than that of the third and fourth sensors, which are closer to the vehicle. As this is not in agreement with the primary assumption that the response of the structure should decrease with increasing distance from the vehicle, these two coefficients will hereafter be neglected. It should be noted that the distance between the two sensors and the overtaking lane is large, which means that the measured values are unreliable; indeed they are extremely low and sometimes even negative.

Table 4: Coefficients after eliminating the data provided by the 8th sensor.

Sensor j	1	2	3	4	5	6	7	9	10	11	12
$\overline{k}_j^1$	0.088	0.927	1.753	0.807	1.321	0.750	1.539	0.853	0.698	0.988	1.503
$\overline{k}_j^2$	5.487	2.794	1.299	0.406	0.748	0.668	1.550	0.962	0.921	1.340	0.858
$\overline{k}_j$	0.088	0.927	1.526	0.607	1.035	0.709	1.545	0.908	0.809	1.164	1.181

Now we need to determine the correction factor for the eliminated sensor, by returning to the individual computations of the basic algorithm without the data relating to the eighth sensor. For the parameters $\beta_1 - \beta_4$ of each computation i ($i = 1,2,\dots, M_1 + M_2$), the function value f_i is calculated using Equation (2) at position x_8, and the quotient

$$k_8(t_i) = \frac{f_i(x_8)}{S_8(t_i)}. \tag{6}$$

The average coefficients of the eighth sensor ($\overline{k}_8^1 = 0.403, \overline{k}_8^2 = 0.390$) are then evaluated for each lane. By averaging them, $\overline{k}_8 = \frac{\overline{k}_8^1 + \overline{k}_8^2}{2} = 0.397$, the individual coefficient for the eighth sensor is determined. The coefficients $\overline{k}_j$, for $j = 1,\dots, N$ serve as scaling factors for each measured record of the corresponding strain gauge. The corrected responses

$$\tilde{S}_1 = \overline{k}_1 \cdot S_1, \tilde{S}_2 = \overline{k}_2 \cdot S_2, \dots, \tilde{S}_N = \overline{k}_N \cdot S_N \tag{7}$$

can be applied directly in the weighing procedure. Although they lead to more accurate weighing results, it was decided to further improve them by the procedure described in the sequel.

On the scaled data (7) nonlinear regression was once again applied, but this time the more detailed model which allows for two peaks was used (3). For each corrected measurement t_i ($i = 1, 2, \dots, M_1 + M_2$) the procedure presented in Section 3.2 is repeated, and the

correction factors are obtained. The final correction factors $\overline{k}_j^*$ are presented in Table 5 and were obtained as a result of the complete procedure.

Table 5: Final correction factors.

Sensor j	1	2	3	4	5	6	7	8	9	10	11	12
$\overline{k}_j^*$	2.02	1.01	1.15	0.58	1.05	0.63	1.45	0.39	0.87	0.82	1.22	1.24

The curves of the average response which apply in the case of the regression function (3), using the coefficients from Table 5, are very similar in shape to those obtained in the case of the regression function (2), using the coefficients from Table 4. In both cases a one-peak curve is obtained, and the error in the measured gross weight of the vehicles has been only slightly reduced. The reason for this lies in the sparse mesh of the sensors, where only one or a maximum of two sensors are positioned between the wheels, see Figure 2. In most cases the maximum response is detected between the wheels, where sensors measure the response due to the effect of two wheels. If there are more sensors between the wheels, then those beneath the centre of the truck would probably capture lower values than those under the wheels, which would result in a response with two peaks.

4 The effect of correction factors on the accuracy of WIM results

In order to demonstrate the effect of correction factors on the accuracy of WIM results, the proposed method was validated using measurement data obtained on the investigated motorway underpass. Over a period of ten months, the SiWIM® [15] system was also used as a pre-selection tool to detect vehicles that are very likely overloaded. During this period, traffic police patrols pulled off the motorway 62 vehicles of different axle configurations and weighed them with portable static weighing pads at a rest area that is located 3 km beyond the bridge, see Figure 6. Although the results of weighing by means of portable scales are less accurate than those obtained at permanently installed weighing

stations, they can nevertheless still be taken as a reference for the estimation of the accuracy of the treated WIM system [5].

Figure 6: The instrumented underpass (left), and the static weighing of vehicles (right).

The first 18 vehicles (observed during the first two days of static measurements) were used to calibrate the system according to the European specification for weigh-in-motion systems [5]. This provided the initial set-up of the system. The remaining 44 vehicles were used to investigate the accuracy of the proposed method. It should be noted that, for the purposes of this study, these two groups could be merged. The vehicles were divided into two groups in order to fulfil the requirements for the calibration procedure and determination of the calibration factors, see [27] and [28]. The averaged lateral distribution curves were compiled independently by averaging the 382 823 and 23 478 lateral distribution curves that were obtained in the case of lanes 1 and 2, respectively.

In order to compare errors in the measured weights of different types of vehicles with different gross weights and axle loads, the relative error, E, of the numerical results was calculated for the 44 vehicles,

$$E_i = \frac{W_{\mathrm{WIM}} - W_{\mathrm{Stat}}}{W_{\mathrm{Stat}}}, \quad \mathrm{i} = 1, 2, \ldots, n, \tag{8}$$

where w_{WIM} is the gross vehicle weight (GVW), the individual axle weights and the axle group weights being calculated with SiWIM® procedure, and w_{Stat} being the static reference values. The axle groups consisted of axles that were spaced up to 1.8 m apart.

The total load corresponding to an individual axle group is equal to the sum of all the axle loads in the group. *n* is the number of all loading cases, i.e. 44 GVW, 54 individual axles and 64 axle groups.

Table 6 summarises the statistical parameters obtained for the 44 vehicles. The weights and the corresponding errors were evaluated for two cases: (i) without correcting the measured data, i.e. by using the measured data directly, and (ii) with the corrected measured data, i.e. data that were obtained after multiplication with the factors given in Table 5.

Table 6: Mean and standard deviation of the relative errors before and after applying the correction factors; *n* is the size of the data sample.

		Uncorrected		After correction	
Criteria	*n*	Mean	Standard deviation	Mean	Standard deviation
Gross Weights	44	-0.0168	0.0535	0.0038	0.0423
Axle Groups	54	-0.0112	0.0705	0.0110	0.0619
Individual Axles	64	-0.0259	0.0641	0.0063	0.0584

In Figure 7 a comparison of the absolute relative errors of the numerically estimated GVW for all 44 vehicles is presented. The absolute errors are sorted by magnitude. The benefit of the proposed algorithm is clear since the average and the most strongly deviating weighing results are substantially improved. The maximum absolute GVW error decreases from 17.7% to 8.4%, and the 95th percentile of the GVW errors decreases from 11.1% to 7.4%. According to the European specifications for weigh-in-motion [5] a significant enhancement of one accuracy class was achieved for all three criteria (GVW, individual axles, and axle groups). The gross weights and the axles groups advanced from class C(15) to B(10). and the individual axles from class B(10) to B+(7).

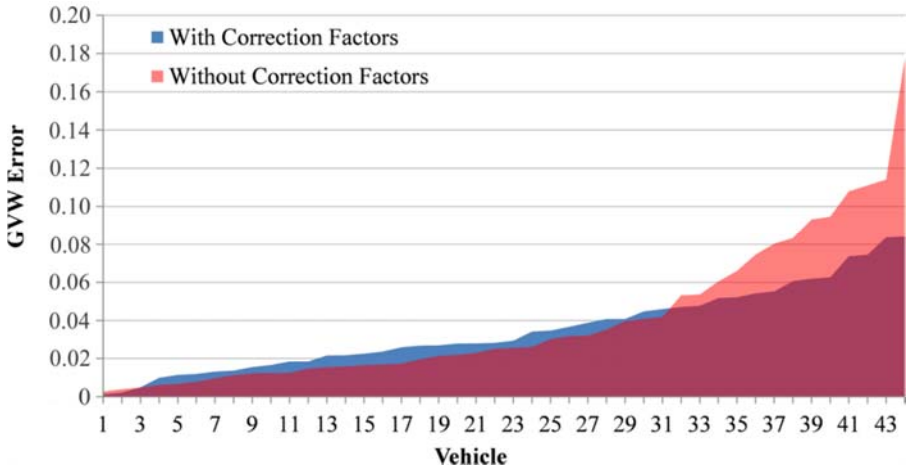

Figure 7: Absolute relative GVW errors sorted by magnitude.

5 Conclusions

The paper presents a novel procedure for the automatic correction of bridge strain response measurements that are used for weighing heavy vehicles in motion. The procedure applies smooth shape functions which approximate well the lateral strain response of the bridge superstructure. One of the key elements of the proposed procedure is its ability to detect sensors with a disproportional response. Based on the assumed and fitted shape functions the correction factors for the measured response were determined. These correction factors notably reduced the errors of the axle and gross weights of the heavy vehicles calculated by the bridge weigh-in-motion system. According to the European specifications for WIM, a significant enhancement of one accuracy class was achieved when the procedure was applied. The procedure is fairly general and can be directly applied to similar concrete reinforced slab bridges with at least two driving lanes. For a more precise shape of the response a denser mesh of sensors is needed.

6 References

[1] D. Cebon, Handbook of Vehicle-Road Interaction, London and New York: Taylor & Francis, 1999.

[2] B. Sivakumar and F. Ibrahim, "'Enhancement of bridge live loads using weigh-in-motion data," *Bridge Structures,* pp. 193-204, 2007.

[3] B. Sivakumar, M. Ghosn and F. Moses, "NCHRP REPORT 683 - Protocols for collecting and using traffic data in bridge design," Transportation Research Board, Washington, D.C., 2011.

[4] FHWA-PL-07-002, Commericial Motor Vehicle Size and Wieght Enforcement in Europe, Washington D.C.: FHWA, 2007.

[5] COST 323, "Weigh-in-Motion of Road Vehicles: Final Report of the COST 323 Action. Jacob, B., OBrien, E.J., Jehaes, S. (Eds.)," LCPC, Paris, 2002.

[6] E. J. OBrien, A. Žnidarič and T. Ojio, "Bridge Weigh-in-Motion – Latest developments and applications world wide," in *5th International Conference on Weigh-in-Motion (ICWIM5). Jacob, B., OBrien, E.J., OConnor, A., Bouteldja, M. (eds.)*, Paris, 2008.

[7] A. Žnidarič, I. Lavrič and J. Kalin, "Nothing-on-the-Road axle detection with threshold analysis," in *Proceedings of the 4th International Conference on Weigh-in-Motion (ICWIM4)*, 2005.

[8] R. E. Snyder, "Field Trials of Low-Cost Bridge WIM," Publication FHWA-SA-92-014, Washington, DC, 1992.

[9] Moses F, "Weigh-In-Motion system using instrumented bridges," *ASCE*

Transportation Engineering Journal, pp. 105: 233-249, 1979.

[10] R. J. Peters, "An Unmanned and Undetectable Highway Speed Vehicle Weighing System," in *Australian Road Research Board Proceedings*, 1987.

[11] WAVE, Bridge WIM - Report of Work Package 1.2, E. J. OBrien and A. Žnidarič, Eds., Dublin & Ljubljana: University College Dublin & ZAG, 2001.

[12] E. OBrien, M. J. Quilligan and R. Karoumi, "Calculating an Influence Line from direct measurements," *Proceedings of the Institution of Civil Engineers, Bridge Engineering 159(1),* pp. 31-34, 2006.

[13] E. J. OBrien, P. Rattigan, A. Gonzales, J. Dowling and A. Žnidarič, "Characteristic dynamic traffic load effects in bridges," *Engineering structures,* p. doi.10.1016, 2009.

[14] ARCHES D16, Recommendations on the use of soft, diagnostic and proof load testing, Brussels: European Commission, http://arches.fehrl.org, 2009.

[15] A. Žnidarič, I. Lavrič and J. Kalin, "Latest practical developments in the Bridge WIM technology," in *Proceedings of the Fifth International Conference on Bridge Maintenance, Safety and Management IABMAS2010*, Philadelphia, USA, 2010.

[16] R. Corbally, M. Kreslin, A. Žnidarič, D. Cantero and J. Kalin, "Technical Specification for the Class A Bridge-WIM System, BridgeMon D1.2 Report," ROD, Dublin, 2013.

[17] R. Corbally, A. Žnidarič, D. Cantero, D. Haijalizadeh, J. Kalin, M. Kreslin, C. Leahy, E. J. OBrien and E. Zupan, "Algorithms for Improved Accuracy of Static Bridge-WIM Systems, D3.1 Report of Bridgemon project," Cestel, Trzin, 2014.

[18] S. Grave, Modelling of Site-Specific Traffic Loading on Short to Medium Span Bridges, Ph.D. Thesis, Department of Civil Engineering, Trinity College Dublin, 2001.

[19] A. González, Development of Accurate Methods of Weighing Trucks in Motion. PhD Thesis, Department of Civil Engineering, Trinity College Dublin, 2001.

[20] A. González, C. Rowley and E. J. OBrien, "A General Solution to the Identification of Moving Vehicle Forces on a Bridge," *International Journal for Numerical Methods in Engineering, 75,* pp. 335-354, 2008.

[21] P. Chatterjee, E. J. OBrien, Y. Y. Li and A. Gonzáles, "Wavelet domain analysis for identification of moving loads from bridge measurements," *Computers & Structures, 84 (28),* pp. 1792-1801, 2006.

[22] A. Žnidarič, I. Lavrič, J. Kalin and B. Kulauzović, SiWIM Bridge Weigh-in-Motion Manual, Fourth edition, Ljubljana: ZAG, Cestel, 2011.

[23] E. J. OBrien, A. Dixon and E. Sheils, Reinforced and Prestressed Concrete Design to EC2: The Complete Process, Second Edition, CRC Press, Taylor & Francis, 2012.

[24] A. Žnidarič, I. Lavrič, J. Kalin and M. Kreslin, "Using strips to mitigate the multiple-presence problem of BWIM systems," in *Proceedings of the 6th International Conference on Weigh-in-Motion (ICWIM6)*, Dallas, Texas, 2012.

[25] MathWorks, "MathLab, http://www.mathworks.com/products/matlab/," 2013. [Online].

[26] O. Rawlings, S. G. Pentula and D. A. Dickey, Applied regression analysis: a research tool — 2nd ed., New York: Springer Verlag, 1998.

[27] B. Jacob, "Assessment of the Accuracy and Classification of Weigh-In-Motion Systems. Part 1: Statistical Background," *International Journal of Heavy Vehicle Systems. 7 (2),* pp. 136-152, 2000.

[28] B. Jacob, E. J. OBrien and W. Newton, “Assessment of the Accuracy and Classification of Weigh-In-Motion Systems. Part 2: European Specification.,” *International Journal of Heavy Vehicle Systems. 7 (2),* pp. 153-168., 2000.